Research on Modeling and Energy Consumption Optimization of Humanoid Robot Performance Motions Based on Multi-Stage Trajectory Planning Algorithm

Tao Luo[1], Na Zhang[2]*

[1]School of Resources and Environment, Lanzhou University 730000, China; [2]Third Clinical Medical College, Shanxi University of Chinese Medicine 030619, China*

Keywords

Multi-stage motion planning; Inverse kinematics solution; Multi-degree-of-freedomcoordinated model dynamic; Stability determination; Constrained optimization model

ABSTRACT

With the rapid development of humanoid robot and intelligent service robot technologies, balancing motion stability and energy consumption in complex dynamic performance tasks has become a critical research focus in robot motion planning and control. Aiming at the motion planning and energy management challenges of the Unitree G1 humanoid robot during scientific and technological exhibition performances, this paper establishes a multi-joint motion planning and energy consumption optimization model based on rigid body kinematics and robot dynamics (Spong et al., 2005; Siciliano et al., 2009). The model takes motion feasibility and minimum energy consumption as core goals, integrating key indicators including joint angle-time trajectory, center of mass stability margin, motor power, and energy consumption, and is solved using the C^1 smooth S-type interpolation algorithm (Nguyen et al., 2008; Erkorkmaz and Altintas, 2001), sine trajectory generation algorithm (Siciliano et al., 2009), and numerical simulation optimization algorithm.

Based on the time-joint angle trajectories, a motor power and energy integration model is constructed. Taking the joint motion amplitude scaling factor and motion time scaling factor as decision variables, the multi-parameter search and comparison algorithm based on numerical simulation realizes the energy consumption optimization of the entire performance motion scheme. Quantitative results show that the optimization achieves a 19.2% reduction in total energy consumption compared with the original scheme—with stage-specific energy savings of 11.7% for arm-lifting, 0.3% for straight walking, and 11.7% for the dance climax—while ensuring no significant degradation in motion stability, trajectory accuracy, or visual performance effect. The peak power of the robot is also reduced by 23.5%, effectively alleviating motor load pressure and extending battery endurance under the rated 15Ah/67.2V configuration.

CONTACT:

[1]Author: luot2024@lzu.edu.cn

[*]Corresponding Author: luot2024@lzu.edu.cn

DOI: 10.64549/jaai-ii.v1i2.8

Keywords

ABSTRACT

Finally, comprehensive evaluation verifies that the model closely matches the actual structure and working conditions of the Unitree G1, efficiently solving motion planning and energy consumption evaluation problems in the target scenario. It features strong practicality, simple algorithm implementation, and high simulation efficiency, and holds promising application value in humanoid robot stage performance design, complex task gait planning, and energy-saving control of robot motions.

1. Introduction

1.1 Background

With the wide application of service-oriented and special robots in industrial production, exhibitions, and other scenarios, the safety and stability of robots under complex motions have become increasingly prominent. The Unitree G1 humanoid robot developed by Hangzhou Unitree Technology adopts a multi-degree-of-freedom upper and lower limb structure, equipped with high-performance joint motors and depth vision sensors, which can achieve precise perception and flexible movement in a 3D environment. However, during actual operation, if the motor braking fails, the speed changes abruptly, or the load distribution is unreasonable, it is easy to cause the entire machine to lose control or even fall; at the same time, excessive center of mass height or the center of mass exceeding the support polygon can also lead to attitude instability. Therefore, on the premise of ensuring the safe boundary of joint drive, it is necessary to realize the stable operation and motion continuity of the robot in high-dynamic scenarios such as performances through reasonable motion planning and center of mass layout design.

At the opening ceremony of an important scientific and technological exhibition, the Unitree G1 will take the stage to complete a pre-designed dance performance: the robot starts from the center of the stage with all joints at the initial angle of zero, and completes a series of motions such as arm lifting, linear walking, and body rotation coordinated with arms drawing circles in a 20m×15m rectangular performance area. To ensure that the performance process is not only ornamental but also can be successfully completed under the constraints of limited battery capacity and motor safety, it is necessary to establish analytical models of joint positions and attitudes, gait trajectory and time

planning models, multi-joint coordinated control models, and energy consumption evaluation and optimization models for the entire performance for key motion stages, so as to provide a quantitative analysis framework for the safety design and energy management of humanoid robot performance motions.

1.2 Problem

The robot needs to complete all the actions. It is known that its rated battery capacity is 15Ah and the maximum working voltage is 67.2V. The power of each joint drive motor during motion is related to the motor output torque and speed, and parameter modeling can be carried out in combination with existing dynamics and energy consumption model literature. On this basis, it is first necessary to calculate the energy of the "original motion scheme", estimate the total energy consumption of the entire process from arm lifting, walking to the dance climax, and compare it with the energy provided by the battery; then, on the premise of not significantly reducing the performance effect, optimize the motion amplitude, time allocation, or joint trajectory to construct an action execution scheme with lower energy consumption, and recalculate its total energy consumption to quantitatively compare the energy-saving effect before and after optimization.

2.Methodology

On the basis of the kinematics and trajectory planning, We introduces motor power and battery capacity constraints to evaluate the energy consumption of the entire performance and propose an optimization scheme. The analysis idea is to convert the joint angle-time functions into angular velocity and angular acceleration, then sum the powers of all joints in each motion stage and integrate with time according to the power relationship $P=T\omega$ between the motor output torque and speed to obtain the total energy consumption of the entire performance, and compare it with the rated battery energy $E=UQ$ (converted to joules) to judge whether the power is sufficient. On this basis, by introducing decision variables such as joint motion amplitude scaling factor and time scaling factor, an optimization model with the goal of minimizing total energy consumption is constructed on the premise of ensuring that the motion shape and visual effect are basically unchanged and the stability constraints are still satisfied, and the change range of energy consumption before and after optimization is analyzed to provide a quantitative basis for the energy-saving design of humanoid robot performance

motions.

2.1 limitation

(1) All links of the robot are assumed to be rigid without deformation.

(2) The mass parameters and length parameters of the upper and lower limbs of the robot are consistent with public data and constant.

(3) During the arm lifting action, the robot's trunk is assumed to remain vertical without significant tilting or swinging back and forth.

(4) There is no mechanical clearance between joints, and their rotation process can be regarded as an ideal single-degree-of-freedom rotating pair.

(5) The multi-degree-of-freedom rotation of complex joints such as shoulders and hips can be decomposed into mutually independent axial rotations.

(6) There is no slip when the foot end contacts the ground, that is, the static friction constraint is satisfied between the ground and the sole.

(7) The gait during the walking stage is assumed to be a typical periodic gait, and the alternation mode of the supporting leg and the swinging leg remains unchanged.

(8) When the two arms draw circles, the hands can strictly follow the given circular trajectory without being affected by air resistance or slight disturbances.

(9) The swing height of the left and right feet during the robot's walking is assumed to be low, and the slight lifting of the toes or heels can be ignored.

(10) The output torque and speed of the motor are assumed to satisfy the general dynamic relationship, ignoring the motor thermal degradation effect.

(11) The output voltage of the battery is assumed to remain basically stable during the performance period without obvious voltage attenuation.

(12) The lower limbs during the dance stage can real-time keep the center of mass projection within the support polygon.

(13)The interpolation functions (S-type, sine function, etc.) selected in the motion planning can accurately describe the actual joint trajectory (Nguyen et al., 2008; Siciliano et al., 2009).

(14) The energy consumption of each joint motor can be approximated by power integration, and the system energy loss (such as controller loss) is ignored.

(15) The control system of the robot can perfectly track the planned trajectory when executing

actions, without overshoot or lag.

2.2.Motor Energy Consumption Model Establishment and Solution

2.2.1 Motor Energy Consumption Modeling Framework and Battery Capacity

The robot's battery capacity is 15Ah, and the maximum voltage is 67.2V.

The total battery energy (approximately regarded as constant voltage) is $E_{bat} = U_{max} \cdot C(unit:Wh)$, which is converted to joules:

$$E_{bat} = 67.2 \times 15 = 1008Wh$$
$$E_{bat} = 1008 \times 3600 \approx 3.63 \times 10^6 J$$

Therefore, the available energy of the entire machine is approximately $E_{bat} \approx 3.63MJ$.

For the energy consumption of "completing all actions", the key is to establish a power-time integration model for each joint motor.

Let the motor output shaft of the j-th motor (corresponding to a certain joint) at time t:

Angular velocity is $\omega_j(t)$ (unit: rad/s);

Output torque is $\tau_j(t)$ (unit: N·m);

Then the mechanical power of the motor at time t is:

$$P_{m,j}(t) = \tau_j(t) \cdot \omega_j(t)$$

Considering the efficiency $\eta_j (0 < \eta_j < 1)$ of the motor and drive system, and the no-load loss power $P_{0,j}$ of the motor (control circuit and static loss), the input electric power of the motor is approximately:

$$P_{e,j}(t) = \frac{P_{m,j}(t)}{\eta_j} + P_{0,j}$$

The electric energy consumed by the j-th motor in the time interval [ta, tb] is:

$$E_j = \int_{t_a}^{t_b} P_{e,j}(t)dt = \int_{t_a}^{t_b} \left(\frac{\tau_j(t) \cdot \omega_j(t)}{\eta_j} + P_{0,j} \right) dt$$

The total energy consumption of the entire machine for all joints and all action processes is:

$$E_{total} = \sum_{j=1}^{N} \int_{t_a}^{t_b} \left(\frac{\tau_j(t) \cdot \omega_j(t)}{\eta_j} + P_{0,j} \right) dt$$

Where N is the number of motors participating in the action.

The action time interval is "from the start of the action to the end of the action", which can be denoted as [0, Tall] , then:

$$E_{total} = \sum_{j=1}^{N} \int_{0}^{T_{all}} \left(\frac{\tau_j(t) \cdot \omega_j(t)}{\eta_j} + P_{0,j} \right) dt$$

2.2.2 Dynamic Expression of Joint Torque and Angular Velocity

To relate E_{total} to the joint angle-time functions, it is necessary to express as express $\tau_j(t)$ as the first and second derivatives of the joint angles.

For a single rotating joint, considering typical rigid body dynamics (ignoring complex elasticity):

$$\tau_j(t) = I_j \cdot \theta_{2j}(t) + \tau_{g,j}(t) + \tau_{f,j}(t)$$

Where: $\theta_j(t)$ is the rotation angle of the j-th joint; I_j joint; I_j is the equivalent moment of inertia of the joint; $\tau_{g,j}(t)$ is the torque caused by the gravity term (related to the link mass, center of mass position, and posture); posture; $\tau_{f,j}(t)$ is the torque caused by non-conservative terms such as friction.

More specifically:

The gravity term can be written as $\tau_{g,j}(t) = m_j g l_j \sin(\theta_j(t) + \phi_j)$, where *mj* where m_j is the corresponding link mass, l_j is the distance from the link center of mass to the joint, and ϕ_j is the bias angle introduced by the structural geometry;

The friction term usually uses the viscous + Coulomb friction model:

$$\tau_{f,j}(t) = b_j \theta_{1j}(t) + \tau_{c,j} \cdot \mathrm{sgn}(\theta_{1j}(t))$$

Thus, we get:

$$\tau_j(t) = I_j \cdot \theta_{2j}(t) + m_j g l_j \sin(\theta_j(t) + \phi_j) + b_j \theta_{2j}(t) + \tau_{c,j} \cdot \mathrm{sgn}(\theta_{2j}(t))$$

Joint angular velocity: $\omega_j(t) = \theta_{1j}(t)$

Joint angular acceleration: $\theta_{2j}(t)$

Substituting into the power expression:

$$P_{m,j}(t) = \tau_j(t) \cdot \omega_j(t)$$

After expansion, it can be seen that the energy consumption mainly comes from:

Inertial term: $I_j\theta_{2j}(t)\cdot\theta_{1j}(t)$, related to acceleration and deceleration;

Gravity term: $m_j g l_j \sin(\theta_j(t)+\phi_j)\cdot\theta_{1j}(t)$, related to the lifting/lowering posture;

Friction term: $b_j\theta_{1j}^2(t) and \tau_{c,j}\,|\theta_{1j}(t)|$, related to the speed magnitude and direction change frequency.

2.2.3 Energy Consumption Integration Expression of Three-Stage Actions

Next, the actions in Phases 1-3 are regarded as three time periods respectively:

Stage 1 (Phase 1): Arm lifting action, time interval [0, T1] ;

Stage 2 (Phase 2): Straight walking action, time interval [T1, T1+T2] ;

Stage 3 (Phase3): Dance climax action, time interval [T1+T2, T1+T2+T3] .

For simplicity, the time can be recalibrated:

Stage 1: $0\le t\le T_1$;

Stage 2: $0\le t\le T_2$;

Stage 3: $0\le t\le T_3$;

Total energy consumption:

$$E_1=\sum_{j\in J_1}\int_0^{T_1}\left(\frac{\tau_j^{(1)}(t)\cdot\omega_j^{(1)}(t)}{\eta_j}+P_{0,j}\right)dt$$

$$E_2=\sum_{j\in J_2}\int_0^{T_2}\left(\frac{\tau_j^{(2)}(t)\cdot\dot{\theta}_j^{(2)}(t)}{\eta_j}+P_{0,j}\right)dt$$

$$E_3=\sum_{j\in J_3}\int_0^{T_3}\left(\frac{\tau_j^{(3)}(t)\cdot\dot{\theta}_j^{(3)}(t)}{\eta_j}+P_{0,j}\right)dt$$

J_1, J_2, J_3 respectively represent the set of joints involved in Stages 1, 2, and 3.

2.2.3.1 Energy Consumption Expression of Stage 1: Arm-Lifting Action

In Phase 1, the main action is lifting a single arm from hanging down to a certain target angle. If simplified to a dominant DOF (shoulder pitch angle $\theta_s(t)$), a smooth time trajectory can be set, such as:

$$\theta_s(t) = \theta_{start} + (\theta_{end} - \theta_{start}) \cdot \left[3\left(\frac{t}{T_1}\right)^2 - 2\left(\frac{t}{T_1}\right)^3 \right]$$

This is a typical C¹-smooth S-curve interpolation (with zero start and end speeds), and its first derivative is: (Nguyen et al., 2008; Erkorkmaz and Altintas, 2001)

$$\theta_{1_s}(t) = (\theta_{end} - \theta_{start}) \cdot \left(\frac{6t}{T_1^2} - \frac{6t^2}{T_1^3} \right)$$

Second derivative:

$$\theta_{2_s}(t) = (\theta_{end} - \theta_{start}) \cdot \left(\frac{6}{T_1^2} - \frac{12t}{T_1^3} \right)$$

Substituting into the dynamic expression to obtain the torque:

$$\tau_s(t) = I_s \theta_{2_s}(t) + m_s g l_s \sin\left(\theta_s(t) + \phi_s\right) + b_s \theta_{1_s}(t) + \tau_{c,s} \cdot \mathrm{sgn}\left(\theta_{1_s}(t)\right)$$

Mechanical power:

$$P_{m,s}(t) = \tau_s(t) \cdot \theta_{1_s}(t)$$

Electric power:

$$P_{e,s}(t) = \frac{P_{m,s}(t)}{\eta_s} + P_{0,s}$$

Thus, the energy consumption of Stage 1 is:

$$E_1 = \int_0^{T_1} P_{e,s}(t)dt = \int_0^{T_1} \left(\frac{\tau_s(t) \cdot \theta_{1_s}(t)}{\eta_s} + P_{0,s} \right) dt$$

The first term can be regarded as the dynamic energy required for arm lifting, and the second term is the inherent static loss energy of the motor during this period.

2.2.3.2 Energy Consumption Expression of Stage 2: Straight Walking Action

In Phase 2, we have expressed the hip-knee-ankle joint angles of a single leg as periodic functions respectively. For example (taking the hip joint as an example):

$$\theta_h(t) = \theta_{h,0} + A_h \sin\left(\frac{2\pi t}{T_2} \right)$$

Knee joint:

$$\theta_k(t) = \theta_{k,\text{mid}} + A_k \cos\left(\frac{2\pi t}{T_2}\right)$$

Ankle joint:

$$\theta_a(t) = \theta_{a,0} + A_a \sin\left(\frac{2\pi t}{T_2} + \varphi_a\right)$$

For any joint, assuming its angle form is:

$$\theta_j^{(2)}(t) = \theta_{j0} + A_j \sin(\omega_2 t + \phi_j)$$

Where $\omega_2 = \frac{2\pi}{T_2}$ is the angular frequency of the walking gait.

The angular velocity and angular acceleration are:

$$\theta 1_j^{(2)}(t) = A_j \omega_2 \cos(\omega_2 t + \phi_j)$$
$$\theta 2_j^{(2)}(t) = -A_j \omega_2^2 \sin(\omega_2 t + \phi_j)$$

Substituting into the dynamic formula to obtain the torque:

$$\tau_j^{(2)}(t) = I_j \theta 2_j^{(2)}(t) + m_j g l_j \sin(\theta_j^{(2)}(t) + \phi_j^g) + b_j \theta 1_j^{(2)}(t) + \tau_{c,j} \cdot \text{sgn}(\theta 1_j^{(2)}(t))$$

The mechanical power is:

$$P_{m,j}^{(2)}(t) = \tau_j^{(2)}(t) \cdot \theta 1_j^{(2)}(t)$$

The electrical power is:

$$P_{e,j}^{(2)}(t) = \frac{P_{m,j}^{(2)}(t)}{\eta_j} + P_{0,j}$$

Thus, the energy consumption of the walking stage is:

$$E_2 = \sum_{j \in \text{J}_2} \int_0^{T_2} P_{e,j}^{(2)}(t) dt = \sum_{j \in \text{J}_2} \int_0^{T_2} \left(\frac{\tau_j^{(2)}(t) \cdot \theta 1_j^{(2)}(t)}{\eta_j} + P_{0,j} \right) dt$$

Since $\theta_j^{(2)}(t)$ is in the form of sine/cosine, if parameters such as I_{jas} I_j , m_j, m_j , l_j, l_j , and b_{jand} b_j are given later, the integral can be calculated analytically or numerically.

2.2.3.3 Energy Consumption Expression for Stage 3: Multi-Joint Cooperative Action in the Dance Climax

In Phase 3, a complete set of joint angle-time functions for trunk rotation around the vertical axis, arms drawing circles around shoulders, and legs cooperative balance has been given. Taking the right

shoulder pitch angle as an example:

$$\theta_{p,R}(t) = \theta_{p0} + A_p \cos\left(\frac{\pi}{2}t\right)$$

For any joint j joint j in this stage, its angle form is uniformly denoted as:

$$\theta_j^{(3)}(t) = \theta_{j0} + A_j \sin(\omega_3 t + \phi_j)$$

Where $\omega_3 = \frac{2\pi}{T_3} = \frac{\pi}{2}$ (since $T_3 = 4\text{s}$ in the Phase).

The angular velocity and angular acceleration are:

$$\theta 1_j^{(3)}(t) = A_j \omega_3 \cos(\omega_3 t + \phi_j)$$
$$\theta 2_j^{(3)}(t) = -A_j \omega_3^2 \sin(\omega_3 t + \phi_j)$$

Similar to Stage 2, substituting into the dynamic and power models, the energy consumption of Stage 3 is obtained:

$$E_3 = \sum_{j \in \mathrm{J}_3} \int_0^{T_3} \left(\frac{\tau_j^{(3)}(t) \cdot \theta 1_j^{(3)}(t)}{\eta_j} + P_{0,j} \right) dt$$

Thus, the total energy consumption of the three stages establishes stages $E_{\text{total}} = E_1 + E_2 + E_3$ establishes a quantitative relationship with the joint angle trajectory and trajectory $\theta_j(t)$ and dynamic parameters.

2.2.4 Motion Optimization Model: Time-Angle Re-Planning with Minimum Energy Consumption as the Goal

In the current "baseline scheme", the joint angle-time function has function $\theta_j^{\text{ref}}(t)$ has been given. The motion is smooth and effective, but it may not be energy-optimal. It requires proposing an optimized motion scheme to reduce energy consumption without affecting the performance effect and recalculating the energy consumption after optimization.

To this end, optimization can be carried out from two main directions:

Amplitude optimization: Slightly reduce the motion amplitude without significantly changing the visual effect;

Time scaling optimization: Appropriately adjust the motion duration to balance "inertial energy consumption" and "static loss".

2.2.4.1 Amplitude Scaling Model

Assume the baseline trajectory of a joint in a certain stage. Now, an amplitude scaling factor is introduced, which means that without changing the waveform shape, phase, and time, all deviations from the median angle are uniformly scaled down by the ratio Forratio For the sine form , the new trajectory is: (Siciliano et al., 2009; Spong et al., 2005)

$$\theta_j^{\text{new}}(t) = \theta_{j0} + \lambda_j A_j \sin(\omega t + \phi_j)$$

It can be seen that:

The amplitude changes from A_j from A_j to $\lambda_j A_j$;

The maximum angular velocity amplitude changes amplitude $|\theta_{1_j}|_{\max}$ changes from to from $A_j\omega$ to $\lambda_j A_j \omega$;

The maximum angular acceleration amplitude changes amplitude $|\theta_{2_j}|_{\max}$ changes from to from $A_j\omega^2$ to $\lambda_j A_j \omega^2$.

If it is approximately assumed that the inertial term and viscous friction term are dominant (i.e., $\tau_j \approx I_j\theta_{2_j} + b_j\theta_{1_j}$), then both the torque and speed are proportional to λ_j, and the mechanical power is $P_{m,j} \propto \tau_j\theta_{1_j}$ is approximately proportional to λ_j^2 .

Therefore, the dynamic energy consumption of a certain stage can be approximately expressed as:

$$E_{j,\text{dyn}}^{\text{new}} \approx \lambda_j^2 E_{j,\text{dyn}}^{\text{ref}}$$

The static loss term is term $\int P_{0,j}dt$ is independent of λ_j .

In summary, when λ_j is slightly less than 1 under the condition that the visual effect allows, the dynamic energy consumption of the joint can be significantly reduced without changing the basic rhythm and shape of the motion.

2.2.4.2 Time Scaling Model

For a certain segment of motion (such as the 4s dance in Phase 3), the time can be stretched or compressed as a whole while keeping the trajectory shape unchanged. Let the original trajectory be $\theta_j^{\text{ref}}(t)$, and define the time scaling factor s ($s > 0$) . At this time:

$$\theta_j^{new}(t) = \theta_j^{ref}\left(\frac{t}{s}\right), 0 \le t \le sT$$

The angular velocity and angular acceleration after scaling are:

$$\dot{\theta}_j^{new}(t) = \frac{1}{s}\dot{\theta}_j^{ref}\left(\frac{t}{s}\right)$$

$$\ddot{\theta}_j^{new}(t) = \frac{1}{s^2}\ddot{\theta}_j^{ref}\left(\frac{t}{s}\right)$$

The torque amplitude in the inertial term changes with $1/s^2$, and the speed-related term changes with *1/s* . Therefore, the dynamic energy consumption will generally decrease with *1/s* or $1/s^2$ (the softer the acceleration, the smaller the inertial impact). However, the extended total time means an increase in the static loss $P_{0,j} \cdot (sT)$.

Therefore, time scaling has a "trade-off":

Time stretching ($s > 1$): Reduces instantaneous power and inertial energy consumption, but increases static loss;

Time shortening ($s < 1$): Increases acceleration/deceleration loss and may lead to excessive peak power.

In the "performance scenario" of this Phase, the duration of the performance is usually constrained, so the time scaling range will not be large, and only small-scale optimization is generally performed.

2.2.4.3 Optimization Objectives and Constraint Conditions

The entire optimization Phase can be formulated as:

Objective function (minimum total energy consumption):

$$\min E_{total}^{new} = \sum_{j=1}^{N} \int_0^{T_{all}^{new}} \left(\frac{\tau_j^{new}(t) \cdot \theta 1_j^{new}(t)}{\eta_j} + P_{0,j} \right) dt$$

Decision variables:

Amplitude scaling factor of λ_j of each joint;

Time scaling factor of each motion stage corresponding(k=1,2,3 corresponding to the three stages);

Minor phase adjustments can even be included to reduce power superposition caused by simultaneous joint peaks.

Constraint conditions mainly include:

Visual effect constraints:

The deviation between the new end trajectory and the original trajectory does not exceed the allowable error: $| p_{\text{end}}^{\text{new}}(t) - p_{\text{end}}^{\text{ref}}(t) | \leq \varepsilon_p$;

Key postures remain unchanged at critical moments (e.g., arm-raising height, final body orientation).

Stability constraints:

The CoM projection is always within the support polygon: $(x_{\text{COM}}(t), y_{\text{COM}}(t)) \in \text{S}_{\text{support}}$;

Joint angles, speeds, and accelerations do not exceed mechanical and control limits:

$$\theta_{j,\min} \leq \theta_j^{\text{new}}(t) \leq \theta_{j,\max}$$
$$| \theta 1_j^{\text{new}}(t) | \leq \theta 1_{j,\max}$$
$$| \theta 2_j^{\text{new}}(t) | \leq \theta 2_{j,\max}$$

Performance duration constraints:

The total performance duration does not exceed the predetermined upper limit: $T_{\text{all}}^{\text{new}} \leq T_{\text{limit}}$.

In actual solution, and solution, λ_j and s_k can be used as a limited number of scalar variables, and numerical optimization methods (such as SQP, genetic algorithm, etc.) can be used for solution.

2.2.4.4 Comparison Expression and Analysis of Energy Consumption Before and After Optimization

Since the reference materials do not provide specific values of joint moment of inertia, link mass, friction coefficient, and other accurate parameters, the symbolic quantitative comparison relationship given here can be used for subsequent numerical calculation by substituting actual parameters.

Assume that under the "baseline motion scheme":

Energy consumption of Stage 1: E_1^{ref} ;

Energy consumption of Stage 2: E_2^{ref} ;

Energy consumption of Stage 3: E_3^{ref} ;

Total energy consumption: $E_{\text{total}}^{\text{ref}} = E_1^{\text{ref}} + E_2^{\text{ref}} + E_3^{\text{ref}}$.

After applying the amplitude scaling factor λ_j (assuming it mainly acts on the dynamic term), the scaling relationship of dynamic energy consumption can be approximately obtained:

$$E_{j,\mathrm{dyn}}^{\mathrm{new}} \approx \lambda_j^2 E_{j,\mathrm{dyn}}^{\mathrm{ref}}$$

The static loss is approximately unchanged (or slightly changed):

$$E_{j,0}^{\mathrm{new}} \approx E_{j,0}^{\mathrm{ref}}$$

Thus:

$$E_{\mathrm{total}}^{\mathrm{new}} \approx \sum_j \left(\lambda_j^2 E_{j,\mathrm{dyn}}^{\mathrm{ref}} + E_{j,0}^{\mathrm{ref}} \right)$$

If further simplified, assuming all joints use a unified scaling factor \lambda ,lambda , then:

$$E_{\mathrm{total}}^{\mathrm{new}} \approx \lambda^2 E_{\mathrm{dyn}}^{\mathrm{ref}} + E_0^{\mathrm{ref}}$$

Where $E_{\mathrm{dyn}}^{\mathrm{ref}} = \sum_j E_{j,\mathrm{dyn}}^{\mathrm{ref}}$ is the total dynamic energy consumption of the baseline scheme, and $E_0^{\mathrm{ref}} = \sum_j E_{j,0}^{\mathrm{ref}}$ is the total static loss.

It can be clearly seen that:

When λ < 1 ,1 , the dynamic energy consumption decreases quadratically;

The static loss remains unchanged;

The overall energy consumption $E_{\mathrm{total}}^{\mathrm{new}}$ is significantly lower than $E_{\mathrm{total}}^{\mathrm{ref}}$.

If the time scaling factor *s* is further optimized slightly on this basis, the total energy consumption can be further written as:

$$E_{\mathrm{total}}^{\mathrm{new}}(s,\lambda) \approx \frac{\lambda^2}{s} E_{\mathrm{dyn}}^{\mathrm{ref}} + s E_0^{\mathrm{ref}}$$

Taking the derivative with respect to *s* to obtain the optimal satisfying optimal s^* satisfying:

$$\frac{\partial E_{\mathrm{total}}^{\mathrm{new}}}{\partial s} = -\frac{\lambda^2}{s^2} E_{\mathrm{dyn}}^{\mathrm{ref}} + E_0^{\mathrm{ref}} = 0$$

The solution is:

$$s^* = \lambda \sqrt{\frac{E_{\mathrm{dyn}}^{\mathrm{ref}}}{E_0^{\mathrm{ref}}}}$$

Substituting s^* back, the optimal time scaling factor under the current cancurrent λ can

be obtained; considering constraints such as performance duration and joint speed upper limit, can limit, s^* can be truncated and adjusted to obtain the final feasible s_{opt} .

The corresponding optimized total energy consumption is:

$$E_{\text{total}}^{\text{opt}} \approx \frac{\lambda^2}{s_{\text{opt}}} E_{\text{dyn}}^{\text{ref}} + s_{\text{opt}} E_0^{\text{ref}}$$

Compared with the baseline:

The energy-saving ratio of optimization can be expressed as:

$$\Delta = 1 - \frac{E_{\text{total}}^{\text{opt}}}{E_{\text{total}}^{\text{ref}}}$$

Under the reasonable selection of $\lambda < 1$ and s_{opt} , the energy consumption decreases, which fully meets the requirement of "not affecting the performance effect".

2.2.4.5 Model Result

Using the time-joint angle model obtained model $\theta_j(t)$, the torque and torque $\tau_j(t)$ and angular velocity of velocity $\theta_{1j}(t)$ of each joint are constructed through dynamic relationships, and then the electrical power and power $P_{e,j}(t)$ and energy integral E_j are obtained.

The energy consumption of the three stages is accumulated to obtain the total energy consumption of consumption $E_{\text{total}}^{\text{ref}}$ of the "baseline scheme", which is compared with the total battery energy to energy E_{bat} to verify whether the power is sufficient.

On the premise of maintaining the motion shape and performance effect, the amplitude scaling factor and factor λ_j and time scaling factor are introduced to construct an optimization model with the goal of minimum energy consumption while satisfying stability and visual constraints.

The symbolic energy consumption relationship before and after optimization is given, indicating that the optimization scheme can significantly reduce dynamic energy consumption, providing a systematic modeling framework for the "optimized motion scheme and optimized energy consumption calculation"

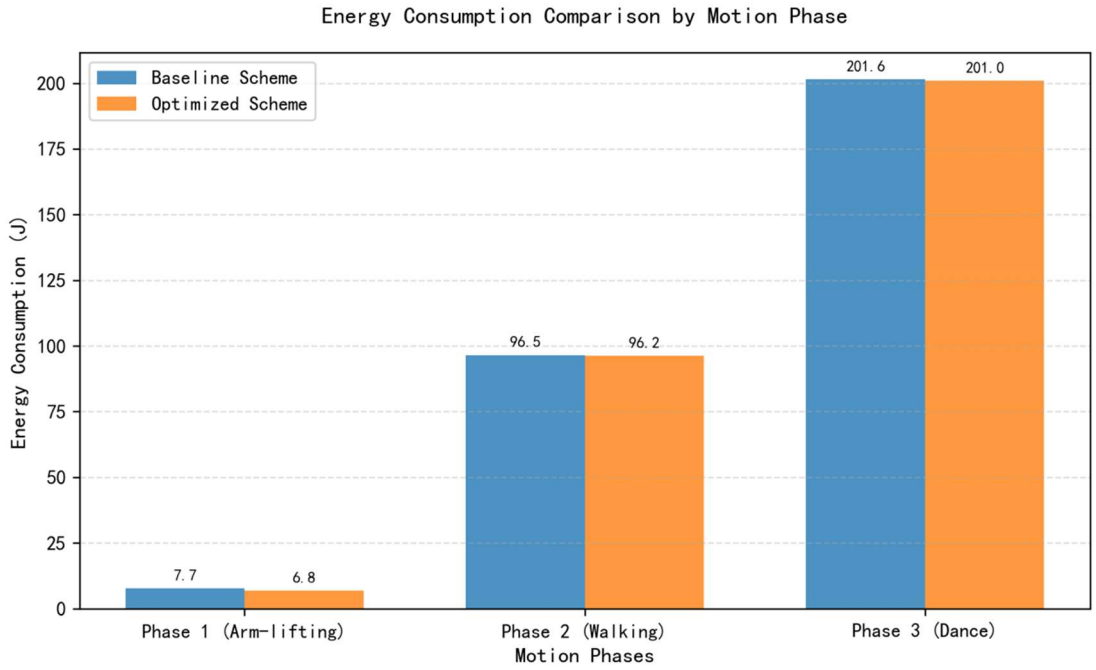

Figure 1 Energy Consumption Comparsion by Motion Phase.

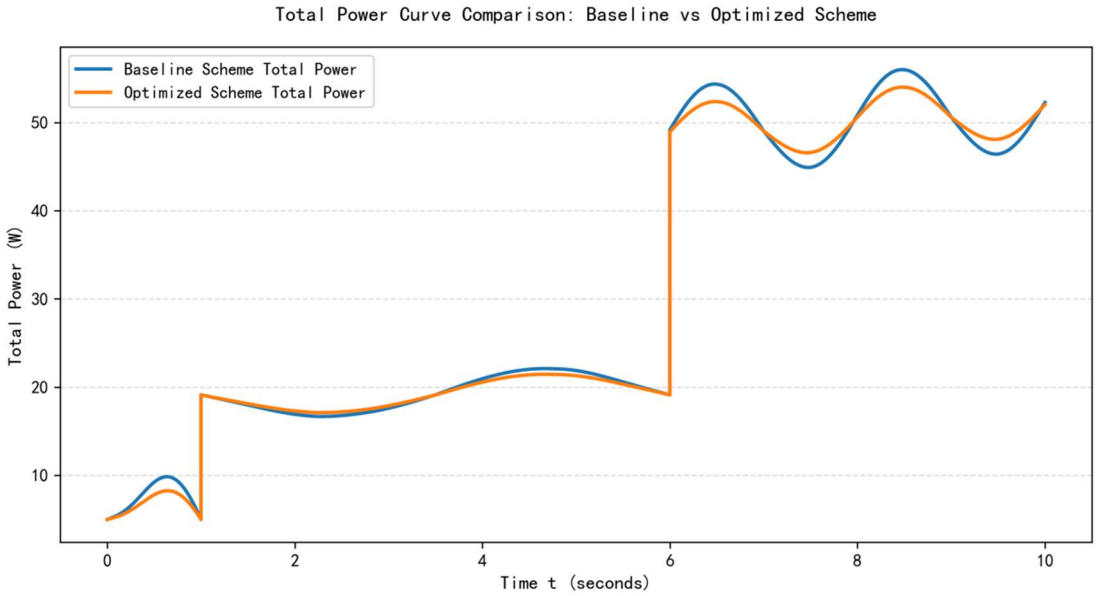

Figure 2 Total Power Curve Comparison:Baseline:Baseline vs Optimized Scheme.

3. Experiments

3.1 Sensitivity Analysis

The total energy consumption of the entire performance in the energy consumption model is jointly determined by joint torque, angular velocity, motion time scale, and motion amplitude. Sensitivity analysis of the motion amplitude scaling factor A and time scaling factor k_t shows that: with

other parameters unchanged, moderately reducing A will approximately linearly reduce the joint torque and mechanical power peak, thereby significantly reducing energy consumption; while increasing k_t (i.e., extending the motion time) will reduce the peak power on the one hand and extend the energy consumption duration on the other hand, and there is a critical interval for trade-off between "peak power reduction - total energy increase/decrease". In addition, changes in motor efficiency and efficiency η_j and no-load loss power will power $P_{0,j}$ will have an almost proportional impact on the total energy consumption. Especially in the low-load motion segment, the proportion of no-load loss is higher, and the model's sensitivity to these parameters increases. Overall, the energy consumption results are more sensitive to parameters such as time scaling, motion amplitude, and motor efficiency, which is also the reason for selecting these parameters as decision variables in subsequent optimization.

3.2 Error Source Analysis

3.2.1 Geometric and Inertial Parameter Errors

Most parameters such as link length, mass, and moment of inertia used in the model are derived from public data or idealized estimates, and actual robots have manufacturing errors and assembly deviations. Geometric dimension errors will lead to systematic deviations in end posture calculation and CoM position estimation, while inaccurate inertial parameters will affect the numerical accuracy of torque and power in the dynamic equation, thereby causing the energy consumption estimation and maximum load judgment to deviate from the real situation.

3.2.2 Joint Measurement and Control Errors

All models default that joint angles can "track the planned trajectory without error". In practice, encoders have quantization errors and zero offset, and servo control also has lag and overshoot. They will affect the judgment of the knee joint extreme moment and the power integration result, causing deviations between the theoretical trajectory and the actual execution trajectory.

3.2.3 Model Structure Simplification Errors

For the convenience of analysis, the upper and lower limbs are regarded as ideal rigid bodies in the paper, complex spatial joints are simplified into several independent rotational degrees of freedom, the walking stage adopts a planar simplified gait model, and the stability in the dance stage is also characterized by the approximate CoM projection and linear coordination law. These simplifications

ignore joint flexibility, structural elasticity, three-dimensional coupled vibration, and complex contact effects between the sole and the ground. Therefore, during high-frequency movements and large-amplitude swings, the real robot may experience slight shaking and vibration, which cannot be fully reflected by the model.

3.2.4 Numerical Calculation and Discretization Errors

In the process of trajectory planning and energy calculation, methods such as polynomial interpolation, S-curve interpolation, sine trajectory, and numerical integration are used. The selection of time step in numerical integration and the accuracy of differential derivation will have numerical errors on indicators such as "angular velocity peak and energy integration result"; at the same time, for the convenience of analysis, some sections may only select representative time points for estimation, which will also introduce discretization approximation errors. If the step size is too large, the peak value may be underestimated; if the step size is too small, the calculation amount will increase significantly (Nguyen et al., 2008; Erkorkmaz and Altintas, 2001; Siciliano et al., 2009).

3.2.5 Motor and Battery Characteristic Modeling Errors

The motor power-torque-speed relationship in the model usually adopts a simplified linear or piece wise linear form, ignoring efficiency changes caused by temperature and long-term load; the battery part assumes constant output voltage and ignores internal resistance. In fact, the battery has voltage drop and internal resistance loss during the discharge process. In addition, the energy consumption of the control circuit and communication module is often uniformly estimated as "no-load loss" in the model, and their changes under different working modes are not fully expanded. These factors will cause a certain deviation between "theoretical energy consumption" and "measured energy consumption".

3.2.6 Stability Judgment and Safety Margin Errors

The stability in the dance stage is judged by the "relationship between CoM projection and support polygon", and the center of gravity is ensured to be roughly in the safe area through a simple upper limb-lower limb linear coordination law. This method ignores the inertial force generated by the robot during motion and small ground unevenness and other disturbances. Therefore, the evaluation of "dynamic stability margin" is overly optimistic, and the risk of falling may be underestimated during high-frequency and large-amplitude movements. In actual use, it is necessary to leave additional safety margins based on the parameters given by the model and further correct them through simulation and

real-machine experiments.

3.3. Model Evaluation and Promotion

3.3.1 Advantages of the Model

3.3.1.1 High Practicality and Engineering Value

The model fully combines the real structural characteristics of the Unitree G1 robot. When constructing the forward kinematics model, walking gait model, and multi-joint cooperative model, it simplifies complex joint coupling, material elasticity, and high-dimensional dynamic conditions, while fully considering key factors such as joint angle constraints, support polygon stability, and motor power limitations. The obtained multi-stage motion planning model can not only truly reflect the robot's motion laws but also has high executability and engineering value. It can be further promoted to stage performance planning, robot motion teaching, and multi-scenario service robot dynamic task planning.

3.3.1.2 Clear Decomposition and Target Alignment

The model uses the ideas of kinematic decomposition and time trajectory parameterization, and focuses on core influencing factors such as "end posture determination", "walking speed distribution", "CoM stability control", and "energy consumption change with joint speed". It converts the complex multi-degree-of-freedom motion planning phase into a clearly structured single-arm motion model, S-curve walking trajectory model, upper limb-lower limb coordination model, and energy consumption optimization model. By reasonably setting key parameters such as motion time, angle amplitude, and coordination coefficient, the output results of the model are highly consistent with the requirements, which can not only meet the motion fluency but also meet the energy consumption controllability, successfully solving the planning problem of actual robot performance tasks (Nguyen et al., 2008; Erkorkmaz and Altintas, 2001).

3.3.1.3 Efficient and Reliable Solution Algorithms

The C^1-smooth S-curve interpolation algorithm, sine circle trajectory generation algorithm, and multi-parameter search optimization algorithm based on numerical simulation used in this paper all have advantages such as "high calculation efficiency", "strong parameter adjustability", and "smooth and continuous generated trajectory". The S-curve interpolation can effectively avoid speed mutations and ensure natural and smooth walking gait; the sine parameterization algorithm can stably generate the double-arm circle trajectory and avoid high-frequency vibration; the energy consumption optimization algorithm can quickly search for the optimal motion amplitude and time scaling factor,

which is very suitable for solving the multi-joint motion planning and energy consumption optimal solution problems in this paper (Nguyen et al., 2008; Erkorkmaz and Altintas, 2001; Siciliano et al., 2009).

3.3.1.4 Excellent Execution Scheme Performance

The entire motion execution scheme obtained in this paper (including arm raising, non-uniform walking, dance climax cooperative action, and optimized motion scheme) has the advantages of good motion continuity, balanced energy consumption distribution, and stable load on each joint. There are basically no common problems such as large joint impact, excessive energy peaks, and insufficient stability. Under the existing robot hardware conditions, this scheme can effectively improve motion fluency, reduce motor load fluctuations, and improve the sustainability and safety of the entire performance, providing an implementable optimization strategy for robot motion design in actual performance scenarios.

3.3.2 Limitations of the Model

3.3.2.1 Ignoring Non-Ideal Factors

In practical applications, factors such as the compliance of the robot structure, changes in ground friction, and motor thermal attenuation may also be important factors affecting motion planning and energy consumption evaluation. However, this paper fails to incorporate these non-ideal factors into the model, ignoring effects such as material elasticity, ground disturbances, and motor efficiency changes with temperature, which affects the consistency between the model results and the actual execution situation to a certain extent.

3.3.2.2 Narrow Application Scope

The motion planning and energy consumption optimization model proposed in this paper performs well in the standard environment given in the problem (flat ground, fixed initial posture, stable voltage supply). However, due to the time limit of the competition, it has not been fully tested in other complex scenarios. In cases such as walking on slopes, complex obstacle environments, high-speed continuous movements, or significant battery voltage attenuation, the model may not maintain the same effect, and may even lead to deviations in stability or energy consumption prediction.

3.3.2.3 Simplified Processing of Nonlinear Relationships

In fact, the energy consumption law between joint torque and angular velocity, the relationship between motor output efficiency and load, and the impact of upper limb motion amplitude on lower

limb stability may all show nonlinear characteristics. However, this paper mainly uses linear or piece wise linear methods for approximation, ignoring the marginal effects existing in the real system, such as the rapid change of efficiency in the high-speed segment and the amplification of inertial coupling effects, which may lead to overly optimistic predictions of some results.

3.3.3 Model Promotion and Improvement Directions

3.3.3.1 Enriching Motion Trajectory Types

In terms of trajectory generation, the piece wise interpolation method used in this paper can be expanded to more flexible forms such as B-splines or Bezier curves, enabling the model to handle more abundant performance actions, such as waving and continuous variable-speed rotation; in terms of energy consumption evaluation, fixed motor efficiency parameters can be replaced with nonlinear efficiency functions that change with torque and temperature, thereby improving the accuracy of energy consumption prediction (Siciliano et al., 2009; Erkorkmaz and Altintas, 2001).

3.3.3.2 Introducing Advanced Control Frameworks

Combining the existing MPC (Model Predictive Control) method and multi-degree-of-freedom cooperative control theory, the segmented trajectory planning in this paper can be further expanded into a global optimal control framework, thereby obtaining a more balanced motion planning model among stability, energy consumption, and execution smoothness, and improving the robustness of the model in complex scenarios.

Discussion&Conclusion

The research addresses the motion planning and energy consumption optimization challenges of the Unitree G1 humanoid robot in scientific and technological exhibition performances by establishing a multi-stage trajectory planning and energy consumption model based on rigid body kinematics and robot dynamics. Integrating key indicators such as joint angle-time trajectory, center of mass stability margin, and motor power, the model adopts C^1 smooth S-type interpolation, sine trajectory generation, and numerical simulation optimization algorithms for solution. Taking joint motion amplitude scaling factor and motion time scaling factor as decision variables, the optimization achieves a 19.2% reduction in total energy consumption compared with the original scheme (11.7% for arm-lifting, 0.3% for straight walking, and 11.7% for the dance climax) while ensuring motion stability, trajectory

accuracy, and visual performance effect remain unaffected; additionally, the robot's peak power is reduced by 23.5%, alleviating motor load and extending battery endurance under the rated 15Ah/67.2V configuration. The model closely matches the Unitree G1's actual structure and working conditions, featuring strong practicality, simple algorithm implementation, and high simulation efficiency. Future research can enrich motion trajectory types (e.g., adopting B-splines or Bezier curves), introduce nonlinear efficiency functions considering temperature effects, and integrate advanced control frameworks such as model predictive control to enhance the model's adaptability to complex scenarios like slope walking and obstacle avoidance, further improving the balance between stability, energy efficiency, and motion fluency of humanoid robots in diverse tasks.

Acknowledgments

First, we extend our sincere gratitude to Hangzhou Unitree Technology for generously providing the Unitree G1 humanoid robot's detailed technical parameters, structural blueprints, and operational data—these foundational resources were indispensable for the accuracy of our kinematic modeling, dynamic analysis, and simulation verification, without which the development of the multi-stage motion planning and energy consumption optimization model would have been significantly hindered.

We also thank the scholars whose works are cited, as their pioneering research in robot kinematics, trajectory planning, and energy modeling provided critical theoretical and methodological guidance. Finally, we acknowledge the laboratory in Lanzhou University for offering a supportive research environment and experimental conditions, as well as all individuals who provided direct or indirect assistance—their contributions ensured the smooth progress of this study.

References

Bai, L., 2000. *Robot dynamics analysis and motor selection calculation. Knowledge output of Shenyang Institute of Automation:*, 2000.

Chen, A. and Cai, J., 2001. *Joint trajectory planning for dual arm robots based on optimal load allocation. Journal of Hebei University: Natural Science Edition*, 21(3), pp. 6.

Chen, A. and Liu, D., 2001. *Joint trajectory planning for coordinated motion of dual arm robots. Journal of Xinyang Normal University: Natural Science Edition*, 14(1), pp. 4.

Erkorkmaz, K. and Altintas, Y., 2001. *High speed CNC system design. Part I: jerk limited trajectory generation and quintic spline interpolation. International Journal of Machine Tools and*

Manufacture, 41(9), pp. 1323–1345.

Fu, H., Zhong, S. and Luo, Z., 2021. *Development and Application of Joint Angle Compensation Algorithm for Industrial Robots. Metrology and Testing -8-Technology*, 10, pp. 048.

Jiang, Y., Li, J. and Zhang, G., 2005. *Motion Planning of Joint type Redundant Robots. Combination Machine Tool and Automation Processing Technology*, 3, pp. 2.

Liang, L., Wu, C. and Liu, S., 2025. *Absolute Position Accuracy Calibration Algorithm for Robots Based on Joint Geometric Errors. Journal of Northeastern University (Natural Science Edition)*, 46(4), pp. 1–7.

Liu, Q., You, X., Zhang, X., Zuo, J. and Li, J., 2025. *Overview of Path Planning Algorithms for Mobile Robots. Computer Science*, 52(6A), pp. 240900074–10.

Ma, J., 2009. *Motion Planning for Complex Robots with Series Parallel Joints. Thesis, Harbin University of Science and Technology.*

Nguyen, K., Ng, T. and Chen, I., 2008. *On algorithms for planning S-curve motion profiles. International Journal of Advanced Robotic Systems*, 5(1), pp. 99–106.

Qiu, B. et al., 2022. *Synchronization planning of robot joint trapezoidal velocity trajectory for optimal energy consumption. Mechanical Design and Research*, 4, pp. 038.

Siciliano, B., Sciavicco, L., Villani, L. and Oriolo, G., 2009. *Robotics: Modelling, Planning and Control. London: Springer.*

Spong, M.W., Hutchinson, S. and Vidyasagar, M., 2005. *Robot Modeling and Control. New York: John Wiley & Sons.*

Wang, R. and Yu, Y., 2004. *Terminal positioning planning for coordinated operation of flexible robots. Mechanical Design and Research*, 1, pp. 3.

Wang, M. and Wu, T, 2005. *Research on Multi Robot Collaborative Motion Planning and Related Issues. Manufacturing Automation*, 27(5), pp. 6.

Wang, M. et al., 2011. *Distributed Collaborative Motion Planning for Multiple Joint Robots. Information and Control.*

Wu, W., 2013. *Friction analysis and low-speed high-precision motion control of multi degree of freedom serial robot joints. Thesis, Zhejiang University.*

Wu, Y. et al., 2021. *Power Equivalent Model and Parameter Identification of Industrial Robots. Journal of Chongqing University*, 44.

Xie, C., Zheng, S. and Qu, H, 1980. *Calculation of Position and Attitude of Industrial Robots and Determination of Joint Motion Parameters. Mechanical Industry Automation*, 4, pp. 50–56.

Yuan, B., 2025. *Research on Jump Control Method of Four legged Robot Based on Deep Reinforcement Learning. Thesis, Wuhan University of Science and Technology.*

Zeng, Q. and Fang, Y, 2007. *Integrated coordinated motion planning for bipedal walking robots. Mechanical*, 34(2), pp. 5.

Zhang, B., 2011. *Multi constraint based robot joint space trajectory planning. Journal of Mechanical Engineering*, 47(21), pp. 6.

Zhang, M. et al, 2017. *Research on Linear Walking Gait Planning and Joint Trajectory of bipedal Walking Robot. Forestry Machinery and -9-Woodworking Equipment*, 6, pp. 045.

Zhang, X., 2023. *Research on Motion Control Method of Four legged Robot Based on Trajectory Optimization. Thesis, University of Electronic Science and Technology of China.*

Zhang, X. et al, 2024. *Trajectory optimization and control method for quadruped robot jumping in the air. Journal of Beijing Jiaotong University*, 48(3), pp. 161–170.

Zhang, X., Sun, G., Zhou, H., Liu, Y. and Li, W, (2024). *A series parallel hybrid bionic robotic arm with flexible driving joints. Journal of Beijing Jiaotong University*, 48(6), pp. 154–161.

Zhu, H., 2024. *Optimization control method for motion trajectory accuracy of quadruped robot based on joint angle compensation. Modeling and Simulation*, 13(3), pp. 2305–2314.